Research Article GU J Sci 38(4): 2033-2044 (2025) DOI: 10.35378/gujs.1420821

Gazi University

Journal of Science

http://dergipark.org.tr/gujs

Production and Characterization of Porous $CaO-Al_2O_3-SiO_2$ (CAS) Glass-ceramics from Eggshell Waste by Sol-gel Method

Zeynep BAYKARA[1], Zafer Yavuz MERKIT[1,*], Bahadır AYDIN[2], H. Ozkan TOPLAN[1], Nil TOPLAN[1]

[1] *Metallurgy and Materials Engineering Department, Engineering Faculty, Esentepe Campus, Sakarya University, 54187 Sakarya, Türkiye*
[2] *Department of Engineering Science, Faculty of Engineering, Istanbul University-Cerrahpasa, 34320 Istanbul, Türkiye*

Highlights

- Porous glass–ceramics with low density and thermal conductivity were made from waste eggshells.
- The addition of Bi_2O_3 showed an encouraging effect on anorthite formation.
- Very low thermal conductivity suggests use in high thermal insulation applications.

Article Info

Received: 17 Jan 2024
Accepted: 30 June 2025

Keywords

Eggshell
Glass-ceramic
CAS
Sol-gel

Abstract

In the present study, the CAS ($CaO-Al_2O_3-SiO_2$) system glass-ceramics were prepared by the sol-gel method using TEOS, $Al(NO_3)_3.9H_2O$, eggshell and HNO_3 as ingredients. The effect of the Bi_2O_3 admixture was comparatively studied to specify the influence on the nucleation and density properties during the glass-ceramic formation. After the drying process of CAS gelation, the powders were calcined at 450°C. To reduce the grain size of the CAS powder, ball milling was carried out using a planetary mill, then heat treatment was carried out as a pellet at 900-1100°C. The crystallization and decomposition temperatures of the dried gel materials were determined using a DTA/TG device. The surface of the porous material was detailed by Scanning Electron Microscope (SEM) for microstructural analysis. The increasing temperature and the addition of Bi_2O_3 had a reducing effect on the appearance of porosity. Density values were calculated by Archimedes method. Temperature and addition of additives caused an increase in density values due to a decrease in porosity. X-ray diffraction (XRD) was used to determine the crystalline phases of the gel powders and heat-treated samples. According to the phase analysis results, it was found that the addition of Bi_2O_3 promoted the formation of anorthite crystals.

1. INTRODUCTION

Glass-ceramics, which exhibit the combined properties of glassy phase and crystalline phase, have been widely investigated in recent years due to their greatly improved physical properties compared to glassy materials. Glass-ceramics are composites that are obtained by controlling the type of crystal phase and grain size structure with heat treatment conditions, by adding compatible composition and nucleating additives to the glassy phase. They have various systems according to their composition types [1,2]. Glass-ceramics based on the $CaO-Al_2O_3-SiO_2$ (CAS) system are commonly used as high plasma-resistant coatings and in solid oxide fuel cells. They are also an important commercial product for building materials [3-5]. The stable phases, such as anorthite ($CaAl_2Si_2O_8$) and wollastonite ($CaSiO_3$), are well-known crystalline phases in $CaO-Al_2O_3-SiO_2$ glass-ceramics [6]. For the intended application, these crystalline phases can be produced by controlling the appropriate temperature, time and initial composition (using different natural raw materials and wastes), taking into account the microstructural properties [7]. In addition to these control groups, fluorides, metal oxides or alkali oxides such as CaF_2, B_2O_3, TiO_2 Bi_2O_3 and Na_2O can be added in order to increase the crystallization tendency. Wollastonite, which is one of the basic stable phases in glass-ceramic systems, is preferred in biomaterial groups such as bone and teeth due to its biological compatibility. Due to their high hardness and corrosion resistance, anorthite group phases find a place in

*Corresponding author, e-mail: zafermerkit@gmail.com

advanced technological applications such as coating surfaces that need wear protection and surfaces in chemical contact and stabilization of nuclear waste [8]. Glass-ceramic materials, which can be produced by crystal formation and growth by heat treatment after forming organic or non-organic glasses traditionally produced by the casting method, can also be produced from precursor glasses obtained by the sol-gel technique [9,10]. The sol-gel technique provides significant advantages in that it can be synthesized by doping various alkoxides, solvents and organic-inorganic molecules, especially around ambient temperature. In addition to allowing glass-ceramic synthesis at lower temperatures compared to traditional glass and ceramic production, the ability to obtain porosity (meso-nano) precursor glass powders with lower grain sizes is a feature that makes this method superior [11]. Porous materials, which can be defined as solid materials containing channels and holes in their structure, can be classified in three different ways: micro, meso and macro, according to pore size [12]. Pore size and distribution of open and closed porosity allow these materials to be used effectively in biomaterial, catalyst, membrane, filter, energy and gas storage applications [13-16]. In addition, it constitutes a preferred material group in advanced aviation applications due to the low density and low thermal conductivity of air trapped in closed pores [17]. It is necessary to work on more environmentally friendly compositions because the solvents and raw materials used in the sol-gel method are economically expensive and polluting in contact with the environment. In the current study, it was aimed to produce porous glass-ceramics with low thermal conductivity in the CAS system by using eggshells as waste raw material.

2. MATERIAL METHOD

In the study, tetraethyl orthosilicate-TEOS (Merck, CAS No. 78-10-4, with ≥99% purity), $Al(NO_3)_3 \cdot 9H_2O$ (Merck, CAS No. 7784-27-2, with ≥98% purity), chicken eggshell (domestic waste), $Bi(NO_3)_3.5H_2O$ (Merck, CAS No. 10035-06-0, with ≥98% purity), Nitric acid (Isolab, CAS No. 7697-37-2, with ≥65% purity) and ethanol (Merck, CAS No. 64-17-5, with ≥99.9% purity) were used. Apart from the composition (CASA) that provides the anorthite-wollastonite formation stoichiometry (57.5 wt%SiO_2, 27.5Al_2O_3, 15CaO) in the CAS ternary equilibrium diagram, the CASB composition was prepared by the sol-gel method, containing 10 wt% Bi_2O_3, in order to improve the crystallization tendency. Table 1 presents the chemical content of the prepared CAS samples, while Table 2 provides the X-ray fluorescence (XRF) analysis of the chicken eggshell before and after calcination.

Table 1. *Chemical composition of the sol-gel synthesized CAS glass-ceramics (wt.%)*

Sample name	CaO	Al_2O_3	SiO_2	Bi_2O_3
CASA	27.5	15	57.5	-
CASB	27.5	15	57.5	10

Table 2. *Chemical composition of raw and calcined chicken eggshell (wt.%)*

Compound	Concentration (wt.%)	
	Raw chicken eggshell	Calcined chicken eggshell
CaO	51.764	97.924
SO_3	0.597	0.246
MgO	0.367	1.044
P_2O_5	0.177	0.317
Fe_2O_3	0.122	0.082
Na_2O	0.110	0.200
SiO_2	0.109	0.061
K_2O	0.083	0.099
Al_2O_3	0.040	0.027

Primitively, the eggshells were ground in a planetary mill at 600 rpm for 10 minutes, and then the powders below 45 μm were reacted with nitric acid to obtain $Ca(NO_3)_2$ After the H_2O:TEOS solution with a mole ratio of 20:1 was dispersed with a magnetic stirrer at 40°C for 1 hour, nitrate compounds were added to provide the CAS stoichiometry determined at the beginning for CASA and CASB compositions, and nitric acid was added at a mol ratio of 3:1 TEOS:HNO_3 as a catalyst. The transparent solution formed was aged

at room temperature to gel for 48 hours. After gelation, the samples were dried at 80°C for 48 hours, calcined at 450°C for 2 hours to remove the nitrates in their structure, and then ground in a planetary mill at 600 rpm for 15 minutes. The powders were pressed with 260 MPa pressure in a cylindrical mold and were applied to heat treatment at 900-1100°C for 1 hour to obtain glass-ceramic by crystallization. In order to determine the crystal phase structure of the powders and heat-treated samples before and after calcination, XRD analysis was examined between 10-80° 2θ degrees at a scanning speed of 2°/min. Microstructure imaging was displayed with the aid of scanning electron microscopy (SEM) using secondary electrons (SE) and backscattered electrons (BES). Thermal conductivity and diffusivity constants of CASA and CASB glass-ceramics were measured using a thermal analyzer, while densities were measured by the Archimedes method. Figure 1 shows schematic representation of the production stages of CAS glass-ceramics.

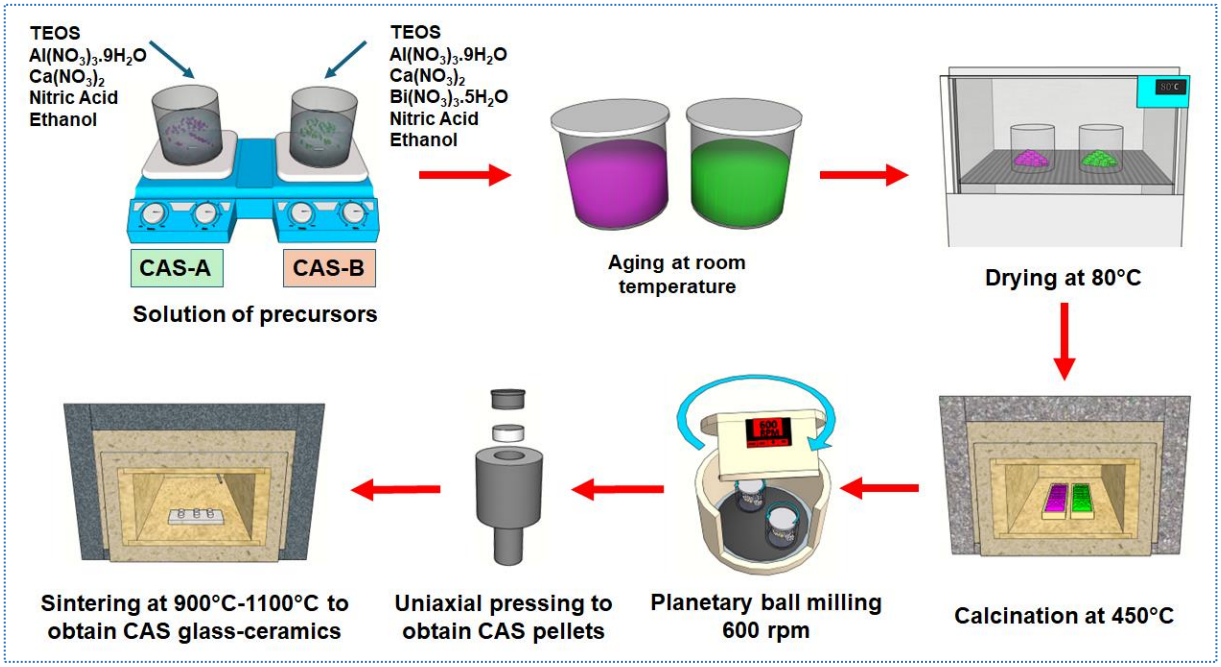


Figure 1. *Schematic representation of the fabrication process of CAS glass-ceramics*

3. THE RESEARCH FINDINGS AND DISCUSSION

3.1. Results of TG-DTA Analysis

The results of the TG-DTA analysis applied to determine the behavior of the base CASA and Bi_2O_3 added CASB composition prepared by the sol-gel method under heat treatment, after aging and drying, are given in Figure 2. Temperature-dependent mass loss occurred gradually at high temperatures up to 500°C for both compositions. It is observed that the water used as TEOS hydrolysis and metal nitrate solvent undergoes dehydration as a result of the endothermic reaction around 99°C [18]. In addition, another mass loss that occurs after the $Al(NO)_3$ decomposition reaction around 200°C is seen in the graph. This decomposition reaction can be expressed by the following equation [19]:

$$Al(NO_3)_3 \xrightarrow{200^oC} \frac{1}{2}Al_2O_3 + \frac{3}{2}NO_2 \quad . \tag{1}$$

In the CASB composition with Bi_2O_3 addition, unlike the composition without additives, a second endothermic curve is observed, expressing the decomposition of $BiONO_3.H_2O$ at ~180°C [20]. The final weight loss for both compounds occurred due to the decomposition reaction of the $CaNO_3$ compound formed by reacting the eggshell with HNO_3 at ~500°C.

According to the results of the DTA analysis applied to determine crystallization temperatures, exothermic peaks corresponding to the crystallization temperature were determined for CASA and CASB at 1030°C

and 1024°C, respectively. For CAS glass-ceramics with similar stichometry, Aydin et al. [21] determined a peak crystallization temperature of 1065°C. In another study using pumice as raw material source, the crystallization temperature was reported as 1011°C [22]. In CAS composition using eggshell as CaO source, the first crystallization temperature 1052°C was reported [23]. In the present study, DTA peaks show similar results with the literature.

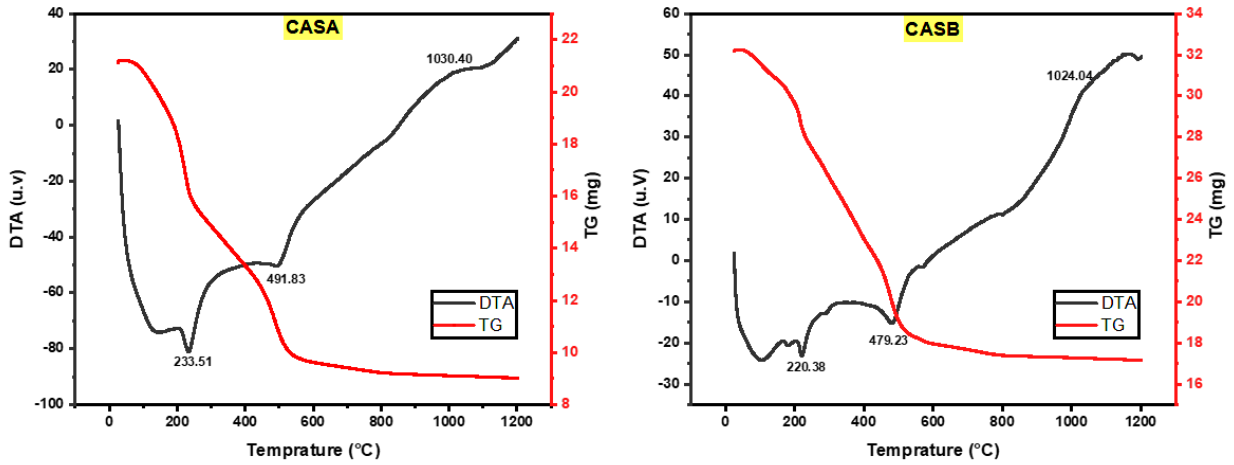


Figure 2. *TG and DTA analysis graphs of CASA and CASB samples prepared by the sol-gel method after aging*

3.2. Results of XRD Analysis

Phase analysis results of CASA and CASB compositions before and after calcination are given in Figure 3. It was observed that the graph of the XRD patterns in CASA composition coincided with the typical amorphous structure before and after calcination.

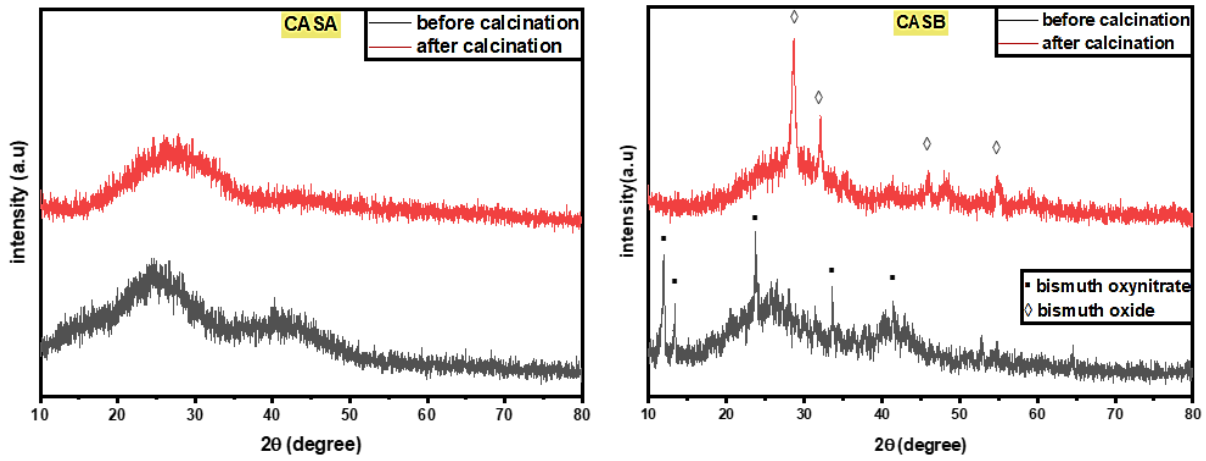


Figure 3. *XRD analysis graphs of CASA and CASB samples before and after calcination*

SiO_2 chain bonds formed after gelation can be shown as the cause of amorphization before dehydration. Although the chain bonds exhibit crystal formation after disintegration after calcination, the grains formed by the sol-gel process are nano-sized and have high nano-porosity, which is the reason no crystal peak is observed after calcination. In the CASB composition prepared by adding $Bi(NO_3)_3.5H_2O$ for the bismuth oxide source, there are peak formations that define a crystalline phase along with amorphization. It corresponds to the bismuth oxynitrate ($Bi_5O(OH)_9(NO_3)_4$) phase formed after the interaction of $Bi(NO_3)_3.5H_2O$ and water before calcination [24]. XRD peaks defining the bismuth (III) oxide phase formed due to the decomposition of bismuth oxynitrate after calcination was seen at various 2θ degrees.

The XRD graphs of the samples applied to heat treatment for 1 hour to obtain glass-ceramic by crystallization at 900-1000°C after calcination are given in Figure 4. A typical XRD pattern showing the formation of an amorphous structure at 900°C is observed for both CASA and CASB samples. The current phase structure of the powders produced by sol-gel is both amorphous and nano porous, which is the main reason for the amorphization as seen in the XRD images after calcination.

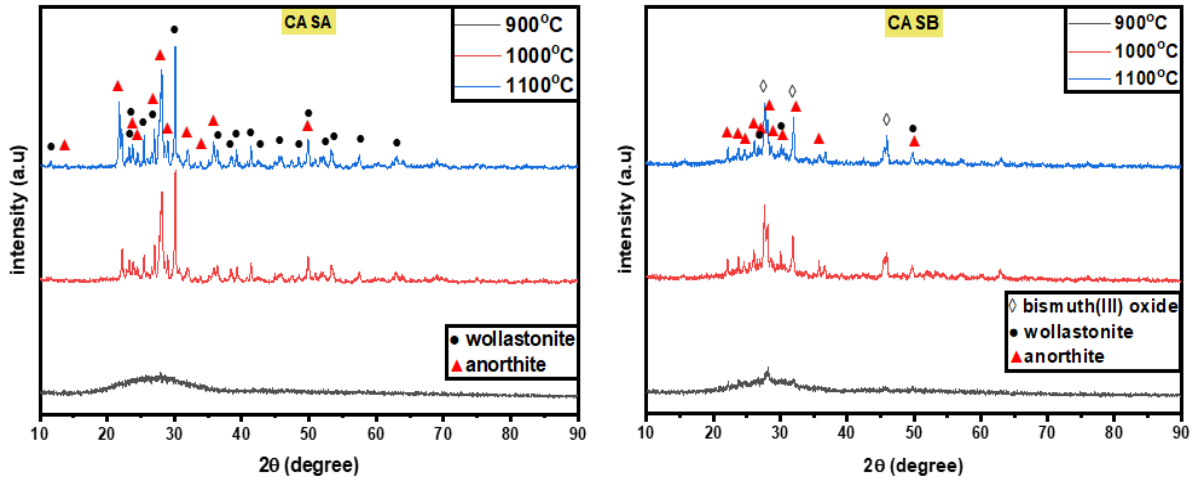


Figure 4. *XRD analysis graphs of CASA and CASB samples after heat treatment*

However, the peak formation corresponding to the low-intensity anorthite (JCPDS 20-0020) phase corresponding to ~27.5 2θ degrees is more prominent for CASB compared to the CASA sample. The existing CAS compositions were prepared according to the CaO-Al_2O3-SiO_2 ternary equilibrium diagram, based on the anorthite-wollastonite formation region with low melting point. In previous studies [25], the initial crystal yield for glass-ceramics synthesized from precursor glasses produced by the traditional glass melting-casting method was obtained at 1000°C for wollastonite. The current situation shows that the addition of Bi_2O_3 in addition to the sol-gel method shifted the initial crystal formation tendency from wollastonite to anorthite. Sol-gel supported glasses have different thermal behavior than melt-casted glasses. In the sol-gel supported method, the low viscosity of the powders due to their hydroxyl content and the increase in free energy with the increasing inner surface reduces the crystallization temperature and accelerate nucleation [26]. When the crystallization temperature is increased to 1000 and 1100 °C, crystal phase formation is clearly observed in CASA and CASB glass ceramics. In the pure CASA composition, wollastonite (JCPDS 19-0248) and anorthite are seen at various 2Θ angles, but anorthite peak intensities are observed to increase at 1100°C. Similar peak intensities were reported in another researcher's CAS study [27]. In CASB glass ceramics with Bi_2O_3 addition, it was determined that some wollastonite phase was formed along with anorthite density at 1000 °C. When the crystallization temperature increased to 1100°C, no significant change in peak intensities was observed. It is noteworthy that in the current study, the Bi_2O_3 compound added as a nucleator appeared at 1000 and 1100 °C because it lowered the crystallization activation energy. It can be said that, due to the low melting temperature of Bi_2O_3, it increases the tendency to form glass with glass precursor powders synthesized with the help of the sol-gel method. This trend is supported by the fact that amorphization does not completely disappear along with crystal formations in the CASB composition. Depending on the percentage of crystal formation, Bi_2O_3 composition began to be seen separating from the glassy phase. As the heat treatment temperature increased, the crystal grain growth and increased crystallization density caused an increase in the peak intensity corresponding to the Bi_2O_3 phase.

3.3. Results of Microstructure Analysis

Figure 5 shows the microstructure images of the powders ground in the planetary mill after calcination. For both compositions, fine-grained powders were formed in submicron size. An inhomogeneous distribution is present in both compositions, with submicron powders forming irregular aggregates in clusters. After the

calcined powders were shaped in a cylindrical mold and subjected to heat treatment between 900-1100°C for 1 hour, SEM images were taken and the results are given in Figure 6.

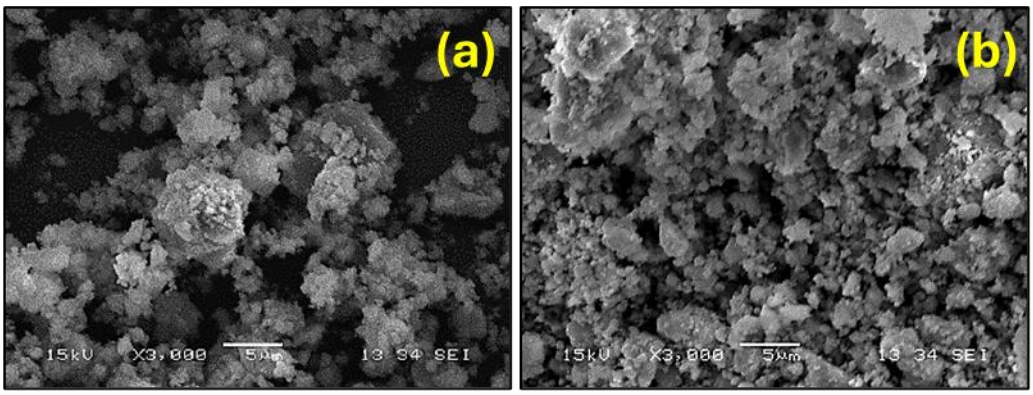


Figure 5*. Microstructure images of a.CASA and b.CASB powders after calcination*

At 900°C, pore structures below 1-20 µm for CASA and CASB composition exhibit a heterogeneous distribution. It can be explained that the pores formed are due to the trapping of NO_2 and O_2 gases in the structure, which are released after the breakdown of $Ca(NO_3)_2$ remaining in the composition. It can be stated that the structure formed at 900°C belongs to an amorphous formation, as indicated in the XRD graph (Figure 4), where no obvious crystal microstructure of any crystalline phase could be detected in the structure. The Bi_2O_3 additive contained in the CASB composition filled the pores formed by forming a liquid phase due to the low melting temperature (817°C), therefore the reticulated pores, which were densely formed in the pure CASA composition, decreased significantly in the CASB composition.

It is seen that the amount of porosity in CASA and CASB samples decreases significantly by increasing the heat treatment temperature to 1000 and 1100°C. Both crystal formation and the growth of the formed crystals can be shown to cause the pores seen at 900°C to decrease at higher temperatures. During heat treatment, the amount of liquid phase increases with increasing sintering temperature, resulting in an increased diffusion rate of the elements forming the matrix throughout the liquid phase [28]. Due to the flux effect of the Bi_2O_3 additive at high temperatures, it reduces the viscosity in the structure and thus the decrease in the amount of porosity has become evident due to its effect on increasing crystal formation and grain growth. The wollastonite phase, whose presence was identified in the ~1µm sized surface morphology showing a wavy appearance for the CASB sample is due to the structure of the anorthite phase. To view the crystal structures formed in detail, SEM-BES images of glass-ceramic samples after heat treatment at 1100°C for 1 hour are given in Figure 7. The light-colored, thin rod-like structures that define wollastonite crystals in the CASA composition exhibit irregular orientations in the glass phase. Light colored distinct regions within the CASB glass-ceramic structure indicate Bi_2O_3 formations distributed within the glass phase. Bi_2O_3, which forms a liquid phase in the glass with heat treatment, has a facilitating effect on atom diffusion by reducing the glass viscosity. As a result, crystal formation began and developed in regions rich in Bi_2O_3 due to the decrease in the activation energy required for anorthite and wollastonite crystallization. Grain growth occurred due to atomic transfer from the glass phase to the grains through diffusion; As the number of atoms forming the anorthite and wollastonite phase decreased in the glass phase, the Bi_2O_3 phase concentrated at the grain boundaries. A similar findings was reported by Khedim et al. [29] in their study of CAS composition with B_2O_3 addition, which had a stoichiometry close to the current study.

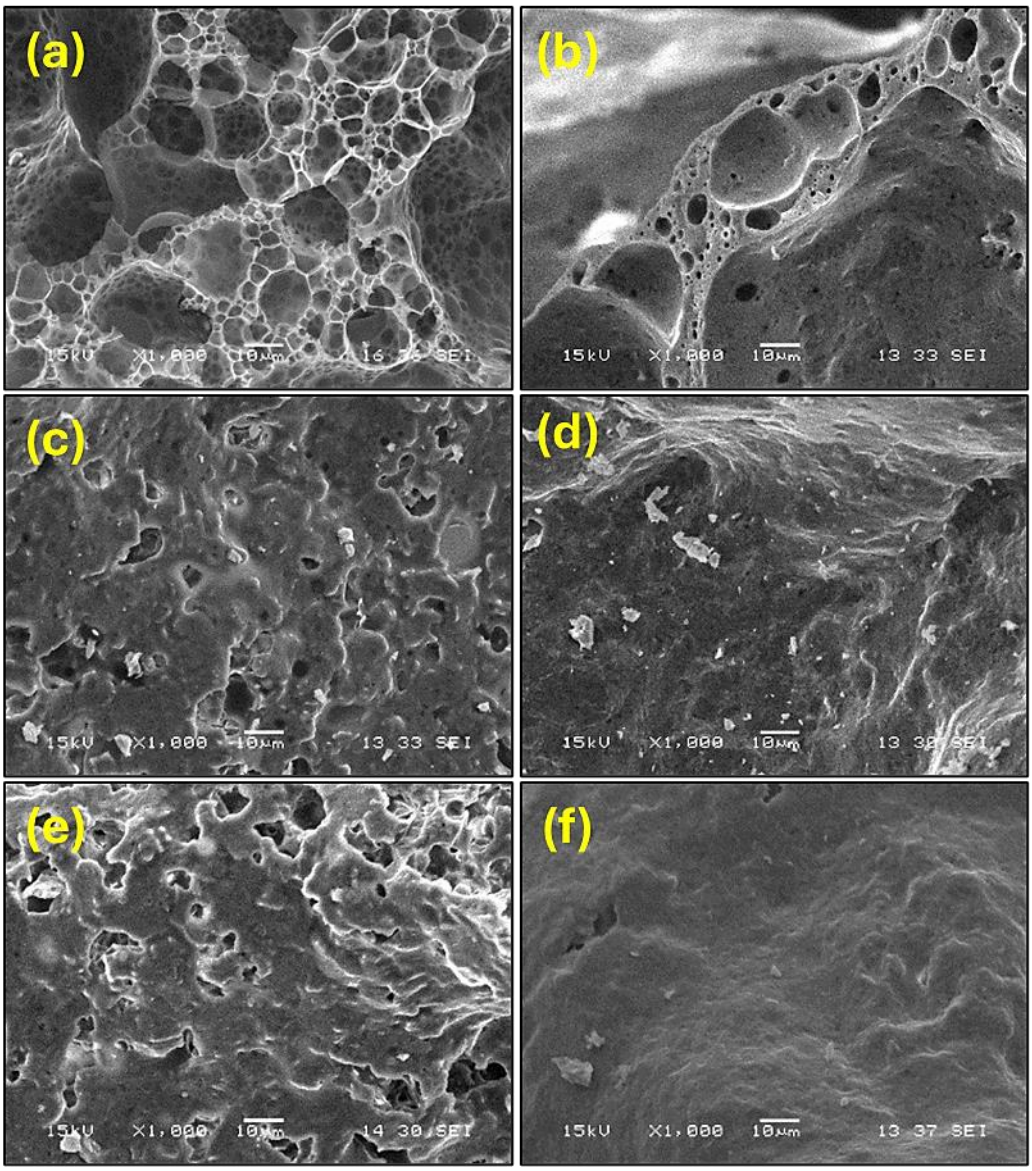


***Figure 6**. Microstructure images of CASA (a.900, c.1000, e.1100°C) and CASB (b.900, d.1000, f.1100°C) glass-ceramics*

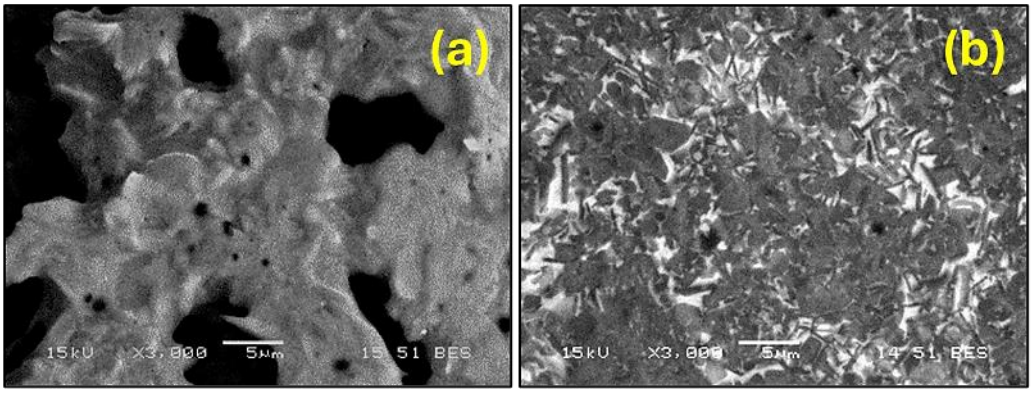


***Figure 7.** SEM-BES microstructure images of a.CASA and b.CASB glass-ceramics crystallized at 100°C*

3.4. Thermal and Physical Properties

Thermal diffusion and thermal conductivity values of glass-ceramic samples were measured at room temperature after the crystallization heat treatment, and the results are given in Figure 8. Thermal diffusion values for CASA glass-ceramic according to different crystallization temperatures are 0.6085, 0.5723 and 0.6076 mm^2/S, respectively; For CASB, it was measured as 0.5348, 0.4713 and 0.5851 mm^2/S. Thermal conductivity values at room temperature are 0.0587, 0.096, 0.074 W/mK for CASA; For CASB, it was measured as 0.074, 0.08517 and 0.076 W/mK, respectively.

Li et al. [30] measured the thermal conductivity values of single-phase anorthite porous ceramics produced by the foam gelation method between 0.04 and 0.27 W/mK, depending on the foaming agent concentration. Xiang et al. also reported that porous anorthite obtained from fly ash waste had a thermal conductivity of 1.24 W/mK [31]. In another study using eggshell waste, Kayalar and his working group [8] reported that they measured a thermal conductivity value of 0.39 W/mK for pure porous anorthite and 0.11W/mK for a composition containing 30% foaming polymer addition. Thermal conductivity is highly related to porosity and pore size. In ceramic materials, heat is transmitted by phonons. As is known, heat is transferred mainly by lattice conduction, and this conduction is achieved through lattice vibration with a specific mode called phonon [32]. While the pores within the material block the heat conduction pathways, the interfaces reduce the cross-sectional area of the heat carried by the phonons. At the same time, the interfacial formation resulting from high pore dispersion and microporosity causes phonon scattering, significantly reducing the thermal conductivity. Small grain size formation causes high interface formation, which is another situation that affects thermal conductivity [33]. In the current study, the fact that the pure CASA composition has the lowest thermal conductivity at 900 °C is directly related to the high porosity of the glass-ceramic sample. Thermal conductivity first increased with the amount of porosity decreasing with the heat treatment, but the thermal conductivity decreased slightly as the grains formed at 1100°C increased the amount of interface. The same situation is also observed for CASB glass-ceramics.

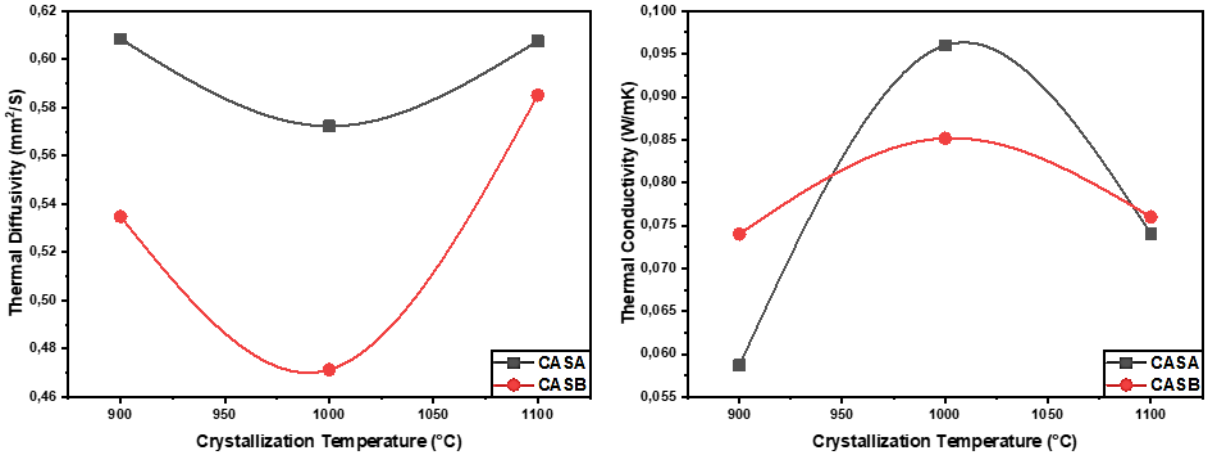


***Figure 8**. Thermal diffusion and thermal conductivity values of CASA and CASB coded glass-ceramics*

The amount of porosity is directly related to density. For this reason, the density measurements of CAS glass-ceramic materials were calculated according to the Archimedes principle and the results are given in the form of a column chart in Figure 9. Density values were measured as 0.114, 0.174 and 0.178 g/cm^3, depending on the increasing heat treatment temperature, for CASA coded glass-ceramic, while for CASB with Bi_2O_3 addition, they were measured as 0.18, 0.226 and 0.193 g/cm^3, respectively. While the lowest density among CASA and CASB compositions was detected in samples heat treated at 900°C; An increase in density is observed as the crystallization heat treatment temperature is increased to 1000°C. However, as the temperature is increased to 1100°C, the CASB glass-ceramic sample exhibits a significant decrease in density, while the density increase is not obvious for the CASA sample. This can be explained by the fact that the porosities present in the material are at their lowest density at 1000°C and the increase in heat treatment temperature creates porosity again for CASB. The increase in density with heat treatment

temperature is due to the softening of the glassy phase. The amorphous structure occupies a larger specific volume than the crystal structure. When the glass is heated to a certain temperature, the volume of the glass first increases, then crystallization occurs, and as a result, the specific volume decreases [34]. Accordingly, as the heat treatment temperature increased at high temperatures, the density of the glass-ceramic increased and, accordingly, its thermal properties decreased. Luo et al. [35] stated that they measured density between 1.42-1.76 g/cm^3 for CAS porous ceramics in their study.

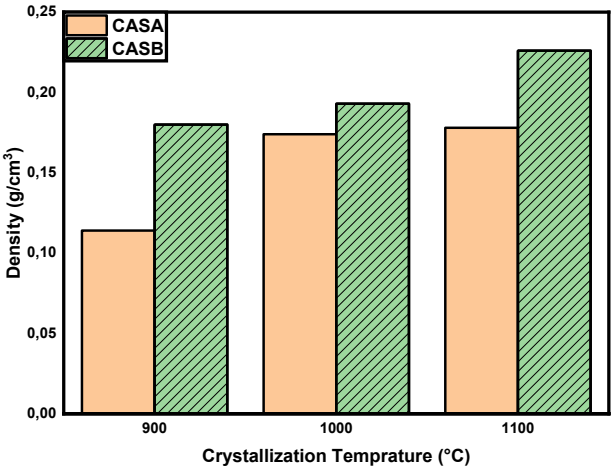


***Figure 9**. Density values of CASA and CAB glass ceramics*

4. RESULTS

In this study, porous glass-ceramics in CAS composition were produced from powders prepared with the help of the sol-gel method, using waste eggshells. The physical and thermal properties of base (CASA) and Bi_2O_3 added (CASB) coded glass ceramics were examined comparatively. It was determined that the phase structure of the powders produced by the sol-gel method was amorphous both before and after calcination at 450°C. However, it has been observed that the presence of bismuthoxynitrate compound, which arises from the reaction of $Bi(NO_3)_3.5H_2O$ compound with water, in CASB powders before calcination, turns into Bi_2O_3 with calcination. Neither composition formed crystals during the heat treatments at 900 °C to obtain glass-ceramic. While the pure CASA composition forms wollastonite and anorthite crystals by increasing the heat treatment temperature, the dominant phase formed by the addition of Bi_2O_3 is anorthite. The porous structure, which was intensely displayed at low temperatures, decreased with increasing heat treatment for both samples. Thermal conductivity values vary between 0.0587-0.096 W/mK for CASA and 0.074-0.08517 W/mK for CASB. The lowest values for both samples were measured at 900°C. The lowest density values were measured as 0.114 and 0.18 g/cm^3 for CASA and CASB, respectively, in samples heat treated at 900°C, similar to thermal properties.

CONFLICTS OF INTEREST

No conflict of interest was declared by the authors.

REFERENCES

[1] Machida, S., Yamaguchi, T., Emori, N., Katsumata, K., Maeda, K., Yasumori, A., "Assessment of the Crystallization Process of CaO-Al_2O_3-SiO_2 Glass Probed with Tb^{3+} Luminescence", Inorganic Chemistry, 61(29): 6-11, (2022). DOI: https://doi.org/10.1021/acsomega.2c08246

[2] Maeda, K., Akatsuka, K., Okuma, G., Yasumori, A., "Mechanical properties of CaO-Al_2O_3-SiO_2 glass-ceramics precipitating hexagonal $CaAl_2Si_2O_8$ crystals", Crystals, 11(4): 1-12, (2021). DOI: https://doi.org/10.3390/cryst11040393

[3] He, F., Zheng, Y., Xie, J., "Preparation and properties of $CaO-Al_2O_3-SiO_2$ glass-ceramics by sintered frits particle from mining wastes", Science of Sintering, 46(3): 353-363, (2014). DOI: https://doi.org/10.2298/SOS1403353H

[4] Ghosh, S., Das Sharma, A., Kundu, P., Mahanty, S., Basu, R. N., "Development and characterizations of $BaO-CaO-Al_2O_3-SiO_2$ glass-ceramic sealants for intermediate temperature solid oxide fuel cell application", Journal of Non-Crystalline Solids, 354(34): 4081-4088, (2008). DOI: https://doi.org/10.1016/j.jnoncrysol.2008.05.036

[5] Jung, Y. S., Min, K. W., Choi, J. H., Yoon, J. S., Im, W. B. and Kim, H. J, "Plasma-resistant characteristics according to sintering conditions of $CaO-Al_2O_3-SiO_2$ glass coating layer", Journal of the Korean Ceramic Society, 59(1): 86-93, (2022). DOI: https://doi.org/10.1007/s43207-021-00149-x

[6] Akatsuka, K., Yasumori, A., Maeda, K., "Structure of crystalline $CaAl_2SiO_8$ precipitated in a $CaO-Al_2O_3-SiO_2$ glass-ceramic", Materials Letters, 242: 163-165, (2019). DOI: https://doi.org/10.1016/j.matlet.2018.12.080

[7] M. Kei, A. Kosho, G. Yasumori, A. Okuma, "Mechanical Properties of $CaO-Al_2O_3-SiO_2$ Glass-Ceramics Precipitating Hexagonal $CaAl_2Si_2O_8$ Crystals", Crystals, 11(4): 393, (2021). DOI: https://doi.org/10.3390/cryst11040393

[8] Torman Kayalar, M., Erdoğan, G., Yavaş, A., Güler, S., Sütçü, M., "Fabrication of porous anorthite ceramics using eggshell waste as a calcium source and expanded polystyrene granules", Journal of Polytech, 900(3): 1235-1241, (2021).DOI: https://doi.org/10.2339/politeknik.911758

[9] James, P.F., "Glass ceramics: New compositions and uses", Journal of Non-Crystalline Solids,181(1): 1-15, (1995). DOI: https://doi.org/10.1016/0022-3093(94)00515-X

[10] Maeda, K., Akatsuka, K., Yasumori, A.,"Practical strength of damage-resistant $CaO-Al_2O_3-SiO_2$ glass-ceramic", Ceramic International, 47(6): 8728-8731, (2021). DOI: https://doi.org/10.1016/j.ceramint.2020.11.236

[11] Kajihara, K., Kanamori, K., Shimojima, A.,"Current status of sol–gel processing of glasses, ceramics, and organic-inorganic hybrids: a brief review", Journal of the Ceramic Society,130(8): 575-58, (2022). DOI: https://doi.org/10.2109/jcersj2.22078

[12] Ibrahim, M. H., Mustaffar, M.I., Ismail, S. A., Ismail, A. N., "A Review of Porous Glass-Ceramic Production Process, Properties and Applications", Journal of Physics: Conference Series., 2169(1), (2022). DOI: https://doi.org/10.1088/1742-6596/1951/1/012007

[13] Kord, M., Marghussian, V.K., Eftekhari-yekta, B., Bahrami, A., "Phase separation, crystallization and leaching of microporous glass ceramics in the $CaO-TiO_2-P_2O_5$ system", Journal of Non-Crystalline Solids, 355 (2): 141-147, (2009). DOI: https://doi.org/10.1016/j.jnoncrysol.2008.10.006

[14] Yuan, H., De Bruijn, J. D., Zhang, X., Van Blitterswijk, C.A., De Groot, K., "Bone induction by porous glass ceramic made from Bioglass® (45S5)", Journal of Biomedical Materials, 58(3): 270-276, (2001). DOI: https://doi.org/10.1002/1097-4636(2001)58:3<270::AID-JBM1016>3.0.CO;2-2

[15] Wu, L., Li, Y., Fu, Z., Su, B. L., "Hierarchically structured porous materials: Synthesis strategies and applications in energy storage", National Science Review, 7(11): 1667-1701, (2020). DOI: https://doi.org/10.1093/nsr/nwaa183

[16] Wu, K., Chen, Z., Li, X., Dong, X., "Methane storage in nanoporous material at supercritical temperature over a wide range of pressures", Nature Scientific Reports, 6(1): 1-10, (2016). DOI: https://doi.org/10.1038/srep33461

[17] Han,Y., Li, C., Bian, C., Li, S., Wang, C. "Porous anorthite ceramics with ultra-low thermal conductivity", Journal of the European Ceramic Society, 33(13-14): 2573-2578, (2013). DOI: https://doi.org/10.1016/j.jeurceramsoc.2013.04.006

[18] Xu, F., Liu, H., Li, D. "Synthesis of PDMS-SiO_2 hybrids using different templates", Journal of Porous Materials, 23: 1133-114, (2016). DOI: https://doi.org/10.1007/s10934-016-0171-6

[19] El-Shereafy, E., Abousekkina, M. M., Mashaly, A., El-Ashry, "Mechanism of thermal decomposition and γ-pyrolysis of aluminum nitrate nonahydrate [$Al(NO_3)_3 9H_2O$]", Journal of Radioanalytical and Nuclear Chemistry, 237(1): 183-186, (1998). DOI: https://doi.org/10.1007/BF02386688

[20] Henry, N., Evain, M., Deniard, P., Jobic, S., Abraham, F., Mentré, O. "$[Bi_2O_2]^{2+}$ layers in $Bi_2O_2(OH)(NO_3)$:synthesis and structure determination", Zeitschrift für Naturforschung B, 60(3): 322-327, (2005). DOI: https://doi.org/10.1515/znb-2005-0315

[21] Aydın, B. Toplan, H.O., Toplan, N. "CaO-Al_2O_3-SiO_2 (CAS) esaslı cam-seramiklerin kristalizasyon kinetiğine farklı hammaddelerin etkisi", Afyon Kocatepe University Journal of Sciences and Engineering Special Issue, 19: 195-203, (2019).

[22] Aydın, B., Toplan, H. O., Toplan, N. "Non-Isothermal crystallization kinetics and properties of CaO-Al_2O_3-SiO_2 (CAS) glass-ceramics from eggshell waste, zeolite and Pumice", Materials, 17(22): 5630, (2024).

[23] Merkıt, Z.Y., Toplan, H.O., Toplan, N., "The crystallization kinetics of CaO-Al_2O_3-SiO_2 (CAS) glass-ceramics system produced from pumice and marble dust", Journal of Thermal Analysis and Calorimetry, 134: 807-811, (2018). DOI: https://doi.org/10.1007/s10973-018-7571-6

[24] Ollevier, T., Jalba, A., Keipour, H. "Bismuth (III) Nitrate Pentahydrate. Encyclopedia of Reagents for Organic Synthesis", 1-9, (2001). DOI: https://doi.org/10.1002/047084289X.rn01981

[25] Merkit, Z.Y., Toplan, H.Ö., Toplan, N.,"The crystallization kinetics of CaO-Al_2O_3-SiO_2 (CAS) glass–ceramics system produced from pumice and marble dust, "Journal of Thermal Analysis and Calorimetry", 34(1): 807-811, (2018). DOI: https://doi.org/10.1007/s10973-018-7571-6

[26] Sales M., Alarcon, J.,"Crystallization of sol-gel-derived glass ceramic powders in the CaO-MgO-Al_2O_3-SiO_2 system", Journal of Materials Science, 30(9): 2341-2347, (1994). DOI: https://doi.org/10.1007/BF01151110

[27] Mukherjee, D.P., S.K., Das, "SiO_2-Al_2O_3-CaO glass-ceramics: Effects of CaF_2 on crystallization, microstructure and properties", Ceramic International, 39(1): 571-578, (2013). DOI: https://doi.org/10.1016/j.ceramint.2012.06.066

[28] Li, B., Qing, Z., Li, Y., Li, H., Zhang, S.,"Crystallization, microstructures and properties of low temperature co-fired CaO-Al_2O_3-SiO_2 glass-ceramic", Journal of Electroceramics, 37(1-4): 145-150, (2016). DOI: https://doi.org/10.1007/s10832-016-0048-8

[29] Khedim, H., Nonnet, H., Mear, F.O.,"Development and characterization of glass-ceramic sealants in the (CaO-Al_2O_3-SiO_2-B_2O_3) system for Solid Oxide Electrolyzer Cells", Journal of Power Sources, 216: 227-236, (2012). DOI: https://doi.org/10.1016/j.jpowsour.2012.05.041

[30] Li, C., Han, Y., Wu, L., Chen, K., L. nan An., "Fabrication and properties of porous anorthite ceramics with modelling pore structure", Materials Letters, 190: 95-98, (2017). DOI: https://doi.org/10.1016/j.matlet.2016.12.131

[31] Xiang, W., Ding, Q., Zhang, G. "Preparation and characterization of porous anorthite ceramics from red mud and fly ash", International Journal of Applied Ceramic Technology, 17(1): 113-121, (2020). DOI: https://doi.org/10.1111/ijac.13148

[32] Kang, Y., Morita, K.,"Thermal conductivity of the CaO-Al_2O_3-SiO_2 System", ISIJ international, 46(3): 420-426, (2006). DOI: https://doi.org/10.2355/isijinternational.46.420

[33] Han, Y., Li, C., Bian, C., Li, S., Wang, C.A., "Porous anorthite ceramics with ultra-low thermal conductivity", Journal of Europian Ceramic Society, 33(13-14): 2573-2578, (2013). DOI: https://doi.org/10.1016/j.jeurceramsoc.2013.04.006

[34] Cheng, T.W., Chen, Y.S., "On formation of CaO-Al_2O_3-SiO_2 glass-ceramics by vitrification of incinerator fly ash", Chemosphere, 51(9): 817-824, (2003). DOI: https://doi.org/10.1016/S0045-6535(03)00189-9

[35] Luo, Z., Liang, H., Qin, C., Zhang, J., Liu, T., Lu, A., "Sintering behavior, microstructures and mechanical properties of porous CaO-Al_2O_3-SiO_2-Si_3N_4 glass-ceramics", Journal of Alloys and Compounds, 773: 71-77, (2019). DOI: https://doi.org/10.1016/j.jallcom.2018.09.231